European Journal of Pharmacology 855 (2019) 124–136

Contents lists available at ScienceDirect

European Journal of Pharmacology

journal homepage: www.elsevier.com/locate/ejphar

Full length article

Role of endothelin-1 clearance in the haemodynamic responses to endothelin-1 in the pulmonary and hindquarter vasculature of anaesthetised rats.

James A. Angus*, Christine E. Wright

Cardiovascular Therapeutics Unit, Department of Pharmacology and Therapeutics, University of Melbourne, Victoria 3010, Australia

ARTICLE INFO

Chemical compounds studied in this article:
Ambrisentan (PubChem CID: 6918493)
Bosentan sodium (PubChem CID: 44387533)
BQ788 (PubChem CID: 3081333)
Endothelin-1 (PubChem CID: 16132423)
Macitentan (PubChem CID: 16004692)
Sarafotoxin S6C (PubChem CID: 16132429)

Keywords:
Endothelin-1
ET_1-Receptor antagonists
Endothelin clearance
Ambrisentan
Bosentan
Macitentan
Sarafotoxin S6C
Pulmonary vascular constriction
Hindquarter vascular constriction

ABSTRACT

In the pulmonary vasculature there is clearance of endothelin-1 from the circulation mediated by endothelin ET_B receptors. This study explored the haemodynamic effects of endothelin-1 and its clearance in the pulmonary and hindquarter vasculature in anaesthetised rats. Carotid and pulmonary artery pressures and pulmonary and hindquarter blood flows were measured. In each rat, a single endothelin-1 or sarafotoxin S6C cumulative dose-response curve was generated with or without antagonist pretreatment (i.v.). Endothelin-1 caused an acute fall in MAP and rise in hindquarter vascular conductance (HVC) followed by a marked increase in MAP at 5 min with falls in HVC and pulmonary vascular conductance (PVC). Bosentan (10, 20 & 30 mg/kg) pretreatment caused dose-dependent inhibition of the MAP increase as well as PVC and HVC decreases to endothelin-1. Similarly, macitentan (30 mg/kg) or ambrisentan (10 mg/kg) caused significant block of responses to endothelin-1. Sarafotoxin S6C caused acute falls in MAP and increases in HVC and then small falls in PVC and HVC, all prevented by pretreatment with ET_B antagonist BQ788 (1 mg/kg). Pretreatment with BQ788 enhanced endothelin-1 potency by 2.5-fold in PVC and 2.4-fold in HVC. With BQ788 and bosentan, the fall in HVC response was completely blocked, but there were residual MAP rises and PVC falls at the highest endothelin-1 dose. Our work confirms the role of ET_B receptors in the pulmonary vasculature that decrease the circulating levels of endothelin-1. This has important consequences in selecting an appropriate ET_A and ET_B dual receptor antagonist to effectively block endothelin-1-mediated pulmonary vasoconstriction.

1. Introduction

Elegant experiments with ^{18}F-labelled endothelin-1 and micro-positron emission tomography in anaesthetised rats confirm that circulating endothelin-1 is bound rapidly to the lung and cleared rapidly from the circulation with $t_{0.5}$ 0.43 min (Johnstrom et al., 2005). Previously it had been shown using a single-pass cumulative tracer technique that 33% of endothelin-1 is extracted by the dog lung *in vivo*; this clearance of endothelin-1 was completely blocked by the ET_B receptor antagonist BQ788, while BQ123 was without effect (Dupuis et al., 1996). Whether this clearance mechanism is sufficient to decrease the haemodynamic effects of an i.v. bolus of endothelin-1 compared with an i.a. bolus injection is controversial (de Nucci et al., 1988; Gardiner et al., 1993). Dual endothelin ET_A and ET_B antagonists raise immunoreactive endothelin-1 plasma levels in rats, rabbits, nonhuman primates and healthy human subjects (Fukuroda et al., 1994; Gratton et al., 1997; Reinhart et al., 2002; Weber et al., 1996). The site of the endothelin-1 clearance mechanism has been suggested to be the lung endothelin ET_B receptors located on endothelial cells from histological evidence and endothelial cell-specific ET_B knockout mice (Kelland et al., 2010). However, there remains the possibility that endothelin ET_B receptors responsible for clearing endothelin-1 could also be located on smooth muscle cells, not only on endothelial cells, as quantitative autoradiography may not have the precision to differentiate at this cellular level.

In rat isolated small pulmonary arteries, in the presence of L-NAME, bosentan the dual endothelin ET_A and ET_B receptor antagonist shifted the endothelin-1 concentration-contraction curve to the left; i.e. bosentan INCREASED the sensitivity to endothelin-1 (Angus et al., 2017a). We concluded that the rat small pulmonary artery reacted to endothelin-1 with a profile consistent with the hypothesis that an endothelin ET_B receptor-mediated clearance of endothelin-1 was functionally effective to limit the local concentration of endothelin-1 available to interact with endothelin ET_A and ET_B receptors that

* Corresponding author.
E-mail addresses: jamesaa@unimelb.edu.au (J.A. Angus), cewright@unimelb.edu.au (C.E. Wright).

https://doi.org/10.1016/j.ejphar.2019.05.009
Received 5 February 2019; Received in revised form 3 May 2019; Accepted 3 May 2019
Available online 04 May 2019
0014-2999/

mediate the contraction of the smooth muscle. We also showed that the endothelin-1 response profile was quite different in rat isolated small mesenteric, tail and main pulmonary arteries where we found no evidence of the purported endothelin ET_B receptor-mediated clearance of endothelin-1 (Angus et al., 2017a).

In the present study, we have specifically measured pulmonary artery conductance and hindquarter vascular conductance in anaesthetised rats to determine the haemodynamic responses to endothelin-1 and sarafotoxin S6c bolus injections (i.v.). Our aim was to determine the pattern of response to endothelin-1 in these two beds *in vivo* in the presence or absence of endothelin receptor antagonists. Our findings are consistent with the hypothesis that the endothelin ET_B receptor-mediated removal of a portion of injected endothelin-1 from the circulation is active in the pulmonary vasculature. This finding may have implications for the choice of endothelin ET_A and ET_B receptor antagonists for the treatment of pulmonary artery hypertension.

2. Materials and methods

2.1. Animals

This study was approved by the University of Melbourne Animal Ethics Committee and performed in accordance with the *Australian code for the care and use of animals for scientific purposes* (8th edition, 2013, National Health and Medical Research Council, Canberra). Male and female Sprague-Dawley rats (300–450 g) were housed at 22 °C with a 12-h light/dark cycle with free access to food and water. Rats were euthanased at the end of experiments with an intravenous (i.v.) overdose of sodium pentobarbitone (Lethabarb, Virbac, Peakhurst, NSW, Australia).

2.2. Surgical preparation

Rats were placed in an induction container and briefly anaesthetised by spontaneous inhalation of 5% isoflurane (Baxter Healthcare, Old Toongabbie, NSW, Australia) in 100% oxygen using an isoflurane anaesthetic vaporiser (Penlon Sigma Delta; Penlon Limited, Abingdon, UK). When lightly anaesthetised, pentobarbitone (60 mg/kg; Troy Laboratories, Glendenning, NSW, Australia) was injected intraperitoneally (i.p.) to induce general anaesthesia. Atropine (1 mg/kg s.c.; Sigma, St Louis, MO, USA) was administered to decrease respiratory secretions and morphine (7.5 mg/kg s.c.; DBL, Hospira, Hamlen, Germany) to aid surgical analgesia. When deeply anaesthetised (no pedal reflex), rats were placed in a supine position on a heat blanket and connected to a pulse oximeter (Physiosuite, Kent Scientific Corp., Torrington, CT, USA). A rectal probe was inserted to monitor body temperature and a Y clip attached to a hind paw to monitor heart rate and oxygen saturation throughout the surgical set-up. Body temperature was maintained at 38 ± 0.2 °C via the Physiosuite heating blanket which adjusts according to rectal temperature.

A tracheotomy was performed and mechanical ventilation provided via a respiratory pump (#7025 Rodent Ventilator, Ugo Basile, Comerio, VA, Italy) throughout the experiment with room air supplemented with 100% oxygen. Stroke volume was set at 6 ml/kg and stroke rate set to ~76 breaths/min and adjusted to maintain arterial pH at 7.4 ± 0.2 as determined by analysis of blood pH, O_2 and CO_2 (ABL5, Radiometer Medical A/S, Copenhagen, Denmark).

The right carotid artery was isolated with 5/0 braided silk ligatures (Ethicon, Bridgewater, NJ, USA) and a clear polyvinyl catheter (ID, 0.50 mm; OD, 0.80 mm) inserted approximately 1–1.5 cm via a small incision in the artery. The catheter was pre-filled with heparinised (10 U/ml; Pfizer, New York, NY, USA) saline 0.9% (Baxter Healthcare). The catheter was connected to a pressure transducer (Argon Medical Devices, Athens, Greece) for the measurement of pulsatile blood pressure, mean arterial pressure (MAP) and heart rate. The transducer was connected via a bridge amplifier to a Powerlab 8SP (AD Instruments Pty Ltd, Bella Vista, NSW, Australia) for data acquisition stored on a computer.

Via a small incision in an inner thigh, the femoral vein was isolated with 5/0 braided silk and a saline-filled polyvinyl catheter (ID, 0.50 mm; OD, 0.80 mm) was inserted and secured with the silk ligatures. Anaesthesia was maintained by pentobarbitone (15–30 mg/kg i.v.) administration via this catheter as required. A similar saline-filled catheter was inserted into a jugular vein when the experimental protocol required concurrent bolus and infusion administration of drugs. The jugular catheter was connected to an infusion pump (Adelab Scientific, SA, Australia) for infusion of L-NAME, when applicable.

A midline incision was made in the lower abdominal wall (approx. 2 cm length), exposing the abdominal aorta and iliac bifurcation. The abdominal aorta was isolated just above the bifurcation and a small Silastic Doppler flow probe (Silastic tubing flow cuff 1.3–1.6 mm, Bioseb, Vitrolles Cedex, France) was placed around the aorta and connected to a Directional pulsed Doppler flowmeter (545C-3 Directional Pulsed Doppler, Bioengineering, The University of Iowa, USA) for the recording of hindquarter flow (kHz) and hindquarter vascular conductance (kHz/MAP mmHg).

A 1.5 cm incision was made on the left side of the chest through the 5th intercostal space and retracted to expose the heart, trunk of the pulmonary artery and the pulmonary artery. The pericardial sac was opened and any visible fat deposits cleared from the pulmonary artery. A bent 25G needle (Terumo Medical Corp., Somerset, NJ, USA) was used to make a small hole in the right ventricle just below the trunk of the pulmonary artery and a slightly bent polyvinyl (ID, 0.50 mm; OD, 0.80 mm) heparinised saline-filled catheter was inserted into the pulmonary artery a distance of 5–10 mm and connected to a pressure transducer for continuous monitoring of pulsatile pulmonary artery pressure and mean pulmonary artery pressure (MPAP). The catheter was held in position on the surface of the ventricle with a small piece of tissue paper and drop of cyanoacrylate glue (Vetbond, 3M, North Ryde, NSW, Australia). A trimmed, gel-lubricated Silastic Doppler flow probe (1.6 mm i.d.; Bioseb) was placed on the pulmonary artery and secured in position with a drop of cyanoacrylate glue (Vetbond) on the outside of the chest wall. The chest was clamped closed and the lungs re-inflated if required. The pulmonary artery flow probe was connected to a flowmeter as above for the recording of pulmonary artery flow (kHz) and pulmonary artery vascular conductance (kHz/MPAP mmHg). Warm Gelfusine (1–1.5 ml i.v.; succinylated gelatin solution 4%, plasma substitute; B. Braun, Bella Vista, NSW, Australia) was administered and the animal allowed to stabilise for 30 min before measurement of baseline haemodynamic parameters.

2.3. Drug treatment protocols

Endothelin-1 (0.01–4 nmol/kg) or sarafotoxin S6c (0.01–1 nmol/kg) was administered as i.v. cumulative bolus doses. Dose-response curves were completed to each agonist alone or in the presence of a pretreatment administered at the start of the protocol. Endothelin-1 pretreatment groups were: bosentan (10, 20 or 30 mg/kg i.v. bolus); BQ788 (1 mg/kg i.v. bolus); BQ788 + bosentan (1 mg/kg and 30 mg/kg, respectively); ambrisentan (10 mg/kg i.v. bolus); macitentan (30 mg/kg i.v. bolus); or L-NAME (0.63 mg/kg bolus and 20 mg/kg/h i.v. infusion). Doses used were guided by the literature and relative potency of the endothelin receptor antagonists ambrisentan and macitentan compared with bosentan.

Sarafotoxin pretreatment groups were: BQ788 (1 mg/kg i.v. bolus); or L-NAME (0.63 mg/kg bolus and 20 mg/kg/h i.v. infusion.

The following time control groups were also completed: vehicle treatment; or L-NAME alone (0.63 mg/kg bolus and 20 mg/kg/h i.v. infusion).

2.4. Drugs

Drugs and suppliers were as follows: ambrisentan (Selleck Chemicals, Houston, TX, USA); bosentan (Selleck Chemicals); BQ788 sodium salt (Cayman Chemical, Ann Arbor, MI, USA); endothelin-1 (Auspep, Parkville, Victoria, Australia); L-NAME (Nω-nitro-L-arginine methyl ester HCl salt; Sigma, St Louis, MO, USA); macitentan (Selleck Chemicals); and sarafotoxin S6C (Auspep).

Endothelin-1 was prepared using 10% N–N'-dimethylformamide (Sigma) and MilliQ water and stored as a stock solution at −20 °C until required. Sarafotoxin S6c was diluted in MilliQ water and stored as a stock solution at −20 °C until required. Bosentan was prepared fresh using a 300 mM glucose solution (Chem-Supply, Gillman, SA, Australia). Ambrisentan and BQ788 were diluted fresh in a 1:1:18 solution (1 part ethanol:1 part cremophor:18 parts sterile saline). Macitentan was dissolved immediately before administration in a solution of 1 part ethanol:3 parts cremophor:16 parts sterile saline. L-NAME was diluted fresh in sterile saline.

2.5. Statistics and analyses

Data are expressed as mean ± S.E.M. from *n* experiments (1 agonist curve ± pretreatment per rat). The haemodynamic variables assessed were mean arterial pressure (MAP, mmHg), mean pulmonary artery pressure (MPAP, mmHg), heart rate (beats/min), pulmonary blood flow (kHz Doppler shift), computed pulmonary vascular conductance (PVC; pulmonary flow/MPAP, kHz/mmHg), hindquarter blood flow (kHz Doppler shift) and computed hindquarter vascular conductance (HVC; hindquarter flow/MAP, kHz/mmHg). Baseline haemodynamic variables were compared between groups with no L-NAME pretreatment by one-way analysis of variance (ANOVA). Values were found to be similar in these groups ($P = 0.13$), so respective baseline data were pooled (Table 1). Similarly, baseline values in groups treated with L-NAME were consistent ($P = 0.61$, one-way ANOVA) and were pooled. Baseline variables were thus compared between the pooled groups untreated or treated with L-NAME by Student's unpaired *t*-test. Graphs were plotted as (i) absolute data and (ii) data calculated as percentage change from baseline taken as 100%. The effects of agonist doses on each haemodynamic metameter were compared using the absolute data within treatment group by repeated measures (RM) one-way ANOVA with Greenhouse-Geisser correction for lack of sphericity and Dunnett's test for multiple comparisons. Haemodynamic data were compared between treatment groups (e.g. ± L-NAME pretreatment) by RM two-way ANOVA with Greenhouse-Geisser correction for lack of sphericity and Sidak's test for multiple comparisons. All statistical analyses and graphing were performed using Prism 8 (GraphPad Software, San Diego, CA, USA).

To compare the shift in potency of the PVC and HVC dose-response lines to endothelin-1 in control (no pretreatment) groups with endothelin-1 responses after pretreatment with BQ788 or BQ788 + bosentan (Figs. 3 and 4), we used symmetrical parallel line assay theory and computed the change in potency with 95% confidence limits (Colquhoun, 1971). To validate this test, orthogonal contrasts were determined for non-parallelism between lines. In each test, deviation from parallelism was not significant ($P > 0.05$) over the doses of endothelin-1 chosen to perform this calculation.

Table 1
Baseline haemodynamic parameters in the absence or presence of L-NAME.

Haemodynamic parameter	Without L-NAME Pooled $n = 47–48$	With L-NAME Pooled $n = 27$
Heart rate (beats/min)	338 ± 3	329 ± 4
Mean arterial pressure (mmHg)	66 ± 1	97 ± 3[a]
Mean pulmonary artery pressure (mmHg)	13 ± 0.3	14 ± 0.5
Pulmonary vascular conductance (kHz/mmHg)	0.371 ± 0.013	0.330 ± 0.014[a]
Hindquarter vascular conductance (kHz/mmHg)	0.074 ± 0.003	0.046 ± 0.002[a]

Values are ± S.E.M. Data in groups with no L-NAME pretreatment were similar ($P = 0.13$, one-way ANOVA) – also, data in L-NAME-pretreated groups were comparable ($P = 0.61$, one-way ANOVA) – therefore, respective group baseline values were pooled. [a]$P < 0.05$, compared with respective Without L-NAME group, unpaired *t*-test.

3. Results

3.1. Time course and baseline metameters

The anaesthetised rats had resting haemodynamic metameters as shown in Table 1 and Fig. 1. The mean resting heart rate was similar to that in conscious rats but the MAP was lower due to the anaesthesia, open chest and administration of morphine; metameters were very stable over time. The mean pulmonary artery pressure shows oscillation consistent with respiratory rate. Following the injection of endothelin-1 there was a rapid acute fall in mean arterial pressure and rise in hindquarter vascular conductance with a peak at 1 min before a second slower phase of hypertension and fall in hindquarter vascular conductance (as shown at 5 min post-injection; Fig. 1). To quantify these results, we have taken readings at 1 min (acute) and 5 min post-injection of endothelin-1 and considered each metameter as % of baseline (100%) taken just prior to injection of the first dose of endothelin-1. Absolute data for MAP, PVC and HVC, as well as changes from baseline (Δ), are shown in Fig. 4.

3.2. Effects of endothelin-1 and bosentan

The initial acute (≈1 min) effects of endothelin-1 were lowering of MAP by 24% at the lowest dose of endothelin-1 (0.5 nmol/kg i.v.; $P = 0.0037$) that coincided with a sharp doubling in HVC (216%, $P < 0.0001$; Fig. 2, left panels). Higher (cumulative) doses of endothelin-1 dose-dependently increased MAP ($P = 0.0019$) without any initial fall. Interestingly, there was no significant change to PVC at this acute time period until the highest endothelin-1 dose of 4 nmol/kg (−17%; $P = 0.0002$, RM 1-way ANOVA). The lowest pretreatment dose of bosentan (10 mg/kg i.v.) blocked the initial fall in MAP ($P = 0.15$ compared with baseline); the increase in HVC was not completely inhibited, but largely attenuated (125%, $P = 0.041$; Fig. 2 left).

After 5 min post-endothelin-1 injection, endothelin-1 caused marked dose-dependent doubling (219%) in MAP and falls in HVC of as much as 81% with endothelin-1 4 nmol/kg (Fig. 2, right panels). The constriction in the pulmonary vascular bed was somewhat less with maximum falls in PVC of 59% at 4 nmol/kg ($P = 0.0072$). Pretreatment for 20 min with bosentan (10, 20 or 30 mg/kg) dose-dependently antagonised all 3 metameters and decreased the slope of the endothelin-1 dose-response curves. The highest dose of bosentan (30 mg/kg) completely antagonised the endothelin-1-mediated falls in PVC and HVC (Fig. 2, right panels); while there still appeared to be a rise in MAP (146%) with 4 nmol/kg of endothelin-1, this did not reach significance ($P = 0.079$, Dunnett test with RM ANOVA of absolute values). The low dose of bosentan (10 mg/kg) was sufficient to completely antagonise the fall in PVC with endothelin-1 4 nmol/kg, but only attenuated the fall in HVC from −81% (control) to −54% ($P = 0.008$; Fig. 2).

3.3. Effects of endothelin-1 with BQ788 and bosentan

In the absence of BQ788 or bosentan pretreatment, the percentage changes from baseline in MAP, PVC and HVC are again shown in Fig. 3 as for Fig. 2 (control). The absolute mean ± S.E.M. values as well as the delta (change in absolute units) values from baseline are given in Fig. 4. Again, in the absence of pretreatment, endothelin-1 at the starting dose of 0.5 nmol/kg caused an acute fall in MAP followed by dose-dependent increases in MAP. The blood pressure responses mimic

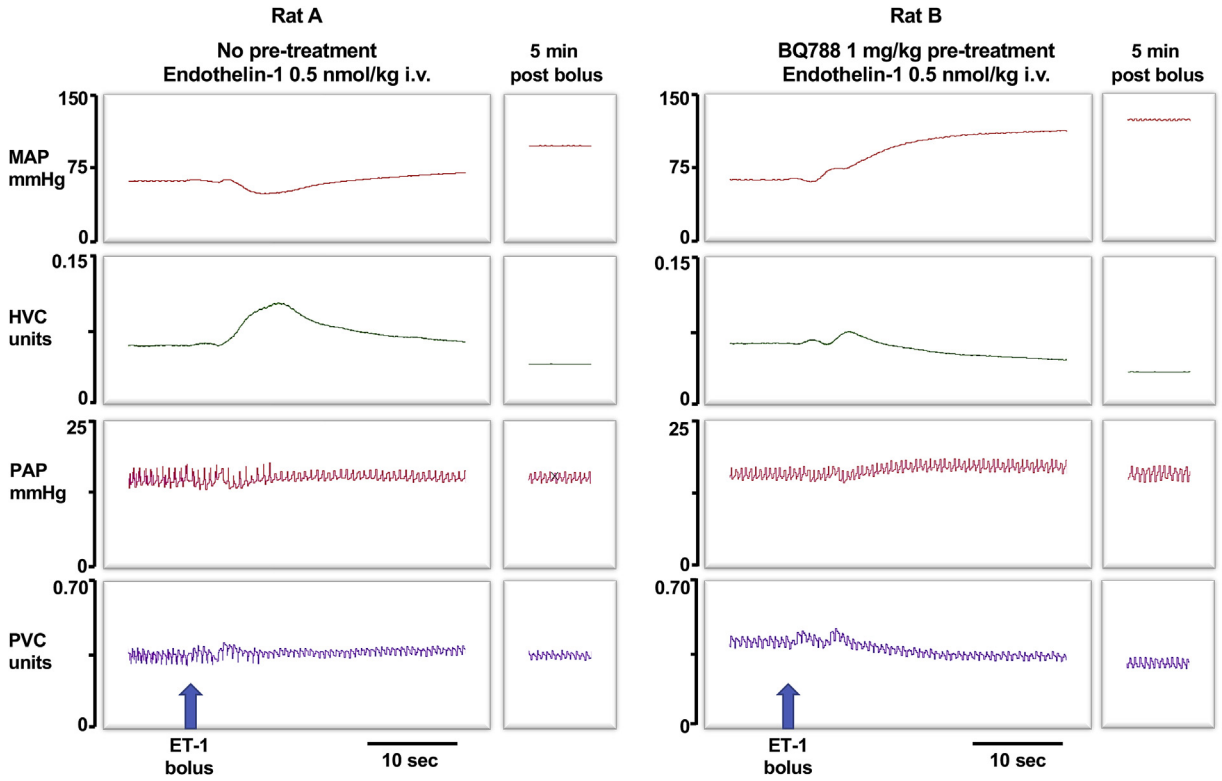

Fig. 1. Typical computer data acquisition recordings from two anaesthetised rats (A and B) in response to an intravenous injection of endothelin-1 (ET-1) 0.5 nmol/kg at arrow. For each rat, there are two recording periods shown: the acute response and the response 5 min post-endothelin-1 bolus. The horizontal bar indicates 10 s. For rat B, the ET_B receptor antagonist BQ788 (1 mg/kg i.v.) was given 20 min prior to the injection of endothelin-1.

directly the increase (216%) and fall (up to −81%) in HVC described in 3.2. After pretreatment with BQ788, there was a marked sensitisation of the pressure/vascular responses where much lower doses of endothelin-1 caused MAP to rise and HVC to fall at the acute (1 min) timepoint (Fig. 3, left panels). These trends at 1 min were replicated and reinforced at the 5 min post-endothelin-1 timepoint. The endothelin-1 dose-increase in MAP relationship was significantly left-shifted (increase in potency) as was the endothelin-1 dose-fall in PVC and HVC relationships (Fig. 3, right panels).

By selecting 2 doses of endothelin-1 in control (2 and 4 nmol/kg) and parallel 2 doses of endothelin-1 in the presence of BQ788 (1 and 2 nmol/kg), we computed the left-shift in the endothelin-1 dose-PVC relationship as 2.53 (95% confidence interval 1.89–3.72) and in the endothelin-1 dose-HVC relationship as 2.37 (95% confidence interval 1.85–3.20), both with no deviations from parallelism ($P = 0.49$ and 0.59, respectively) (Colquhoun, 1971). In separate rats, pretreated with both BQ788 (1 mg/kg) and bosentan (30 mg/kg), the 5 min response for the endothelin-1-mediated increase in MAP was markedly antagonised by approximately 100-fold, with only the 4 nmol/kg dose having a significant effect of +151% compared to baseline (+26 ± 5 mmHg, $P = 0.035$, RM ANOVA with Dunnett's test; Figs. 3 and 4, top right panels). The HVC response was completely blocked at 5 min. In contrast, the PVC 5 min response was right shifted by 4.06-fold (95% confidence interval 2.81–8.98) in a 2 + 2 parallel assay calculation ($P = 0.27$, deviation from parallelism) suggesting that the combination of BQ788 and bosentan was least effective in the pulmonary vasculature.

3.4. Effects of sarafotoxin S6C and BQ788

The selective ET_B receptor agonist sarafotoxin S6C (0.1, 0.5 and 1 nmol/kg i.v.) given as cumulative bolus injections caused acute falls in MAP ($P < 0.0001$) and marked hindquarter vasodilatation as HVC rose to 162 ± 10% ($P = 0.0013$), 191 ± 13% ($P = 0.0004$) and 142 ± 11% ($P = 0.027$) with 0.1, 0.5 and 1 nmol/kg, respectively (Fig. 5, left panels). However, by 5 min post-injection the MAP was dose-dependently slightly elevated ($P = 0.0006$) and HVC had returned to baseline ($P = 0.23$; Fig. 5, right panels). In the pulmonary vasculature, there was no major change to PVC other than a significant fall at both acute (−25%; $P = 0.0044$) and 5 min (−24%; $P = 0.012$) time points with sarafotoxin S6C at 1 nmol/kg.

Pretreatment with BQ788 (1 mg/kg) abolished the sarafotoxin S6C-mediated acute fall in MAP ($P = 0.062$, baseline compared with doses) and increase in HVC ($P = 0.11$) observed in the control rats. With the agonist at 1 nmol/kg, there was still an acute small fall in PVC (−12%; $P = 0.021$) in the presence of BQ788, but this was only half that observed in the absence of the antagonist ($P = 0.023$; Fig. 5). In the presence of BQ788, there were no significant changes in MAP ($P = 0.22$), PVC ($P = 0.054$) or HVC ($P = 0.25$) at 5 min post-sarafotoxin S6C (Fig. 5, right panels).

3.5. Effects of macitentan on responses to endothelin-1

In control group rats, the endothelin-1 responses in Fig. 6 have been repeated again as shown in Figs. 2 and 3. Note the pulmonary vasoconstriction (fall in PVC) at 5 min after administration of endothelin-1 2 and 4 nmol/kg. After macitentan pretreatment (30 mg/kg) in separate rats, the MAP, PVC and HVC acute and 5 min responses to endothelin-1 were completely blocked (each metameter, $P > 0.05$ each agonist dose compared with respective baseline values, RM ANOVA; Fig. 6).

3.6. Effects of ambrisentan on responses to endothelin-1

Ambrisentan (10 mg/kg) pretreatment prevented the acute responses in MAP and PVC following endothelin-1 bolus doses of 0.5–4 nmol/kg, however, there were still small but significant increases

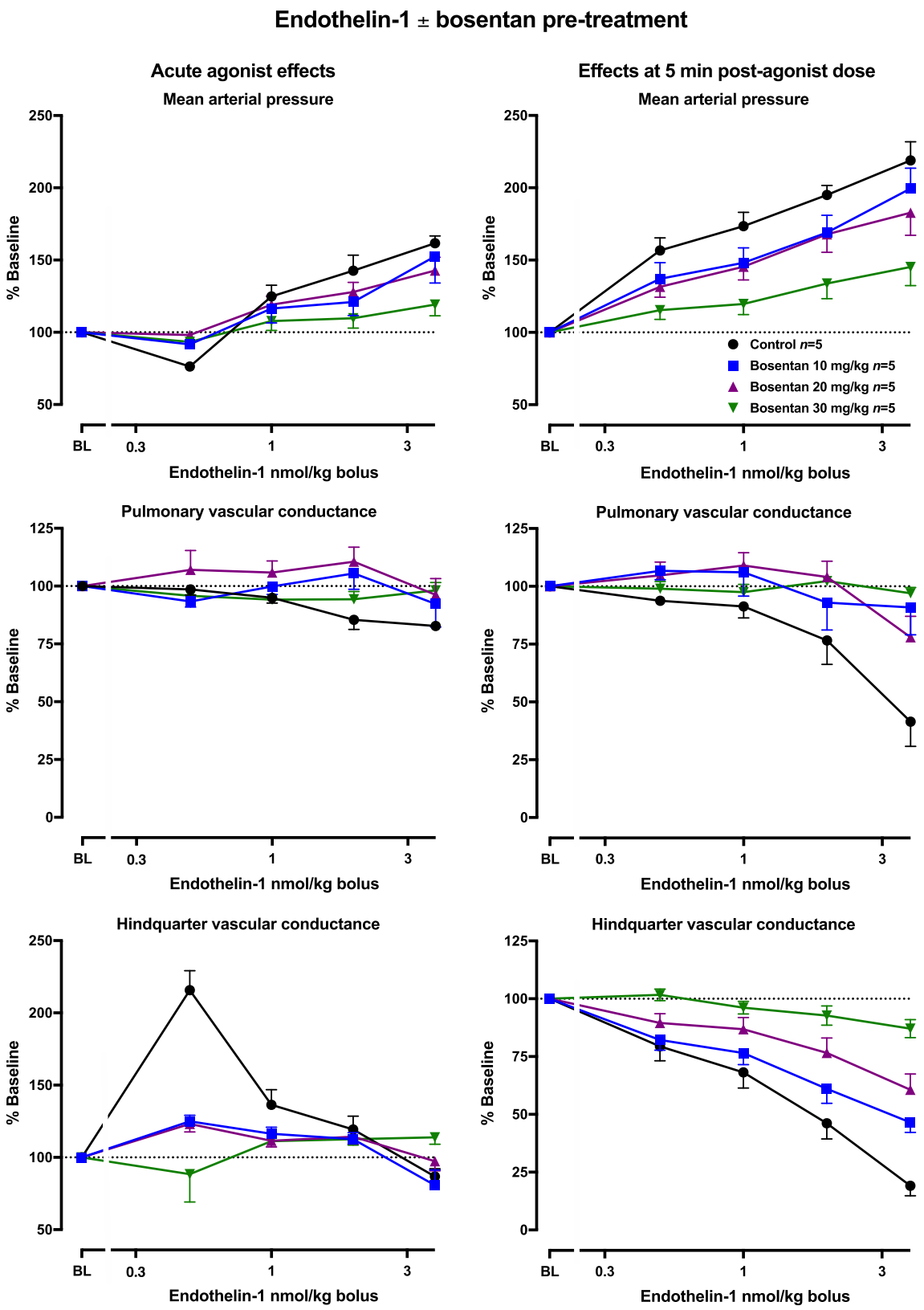

Fig. 2. Effects of the ET_A/ET_B receptor antagonist bosentan on the mean arterial pressure (top panels), pulmonary vascular conductance (middle panels; pulmonary blood flow/pulmonary artery pressure) and hindquarter vascular conductance (bottom panels; hindquarter blood flow/mean arterial pressure) responses to cumulative i.v. bolus injections of endothelin-1 (log scale, x axes). Left panels: Acute (≈0.5–1 min) peak responses to each endothelin-1 bolus dose. Right panels: Measurements at 5 min post-endothelin-1 dose. There are 4 rat treatment groups (n = 5 each; pretreatments administered i.v. 20 min before the first endothelin-1 dose): Control (no pretreatment); bosentan 10 mg/kg; bosentan 20 mg/kg; and bosentan 30 mg/kg. Responses are shown as mean ± S.E.M., calculated as a percentage (%) of baseline (BL) values measured just before injection of the first dose of endothelin-1.

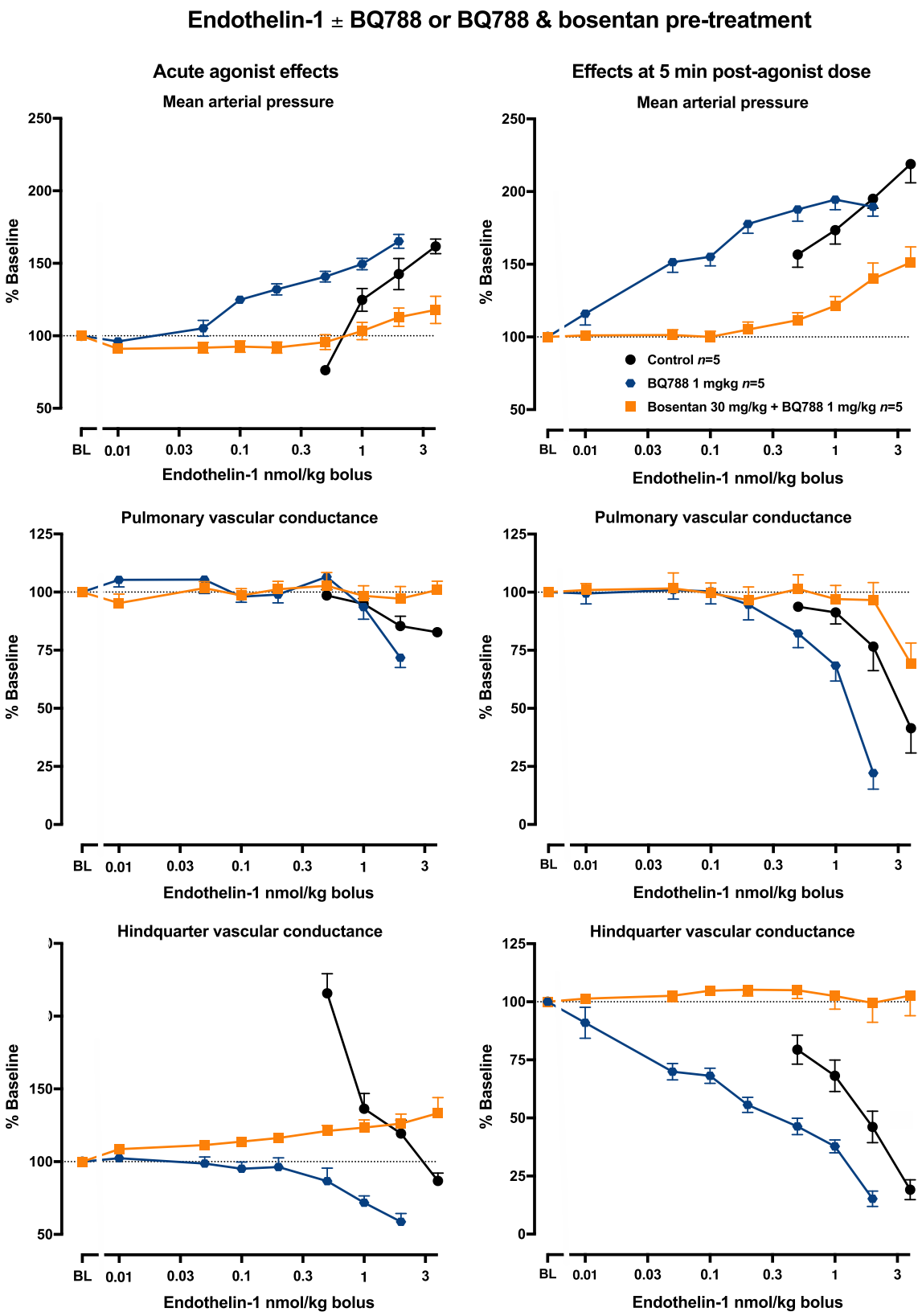

Fig. 3. Effects of the ET_B receptor antagonist BQ788 alone or in combination with bosentan on the mean arterial pressure (top panels), pulmonary vascular conductance (middle panels; pulmonary blood flow/pulmonary artery pressure) and hindquarter vascular conductance (bottom panels; hindquarter blood flow/mean arterial pressure) responses to cumulative i.v. bolus injections of endothelin-1 (log scale, x axes). Left panels: Acute (≈0.5–1 min) peak responses to each endothelin-1 bolus dose. Right panels: Measurements at 5 min post-endothelin-1 dose. There are 3 rat treatment groups (n = 5 each; pretreatments administered i.v. 20 min before the first endothelin-1 dose): Control (no pretreatment; data repeated from Fig. 2 for comparison); BQ788 1 mg/kg; and BQ788 1 mg/kg combined with bosentan 30 mg/kg. Responses are shown as mean ± S.E.M., calculated as a percentage (%) of baseline (BL) values measured just before injection of the first dose of endothelin-1.

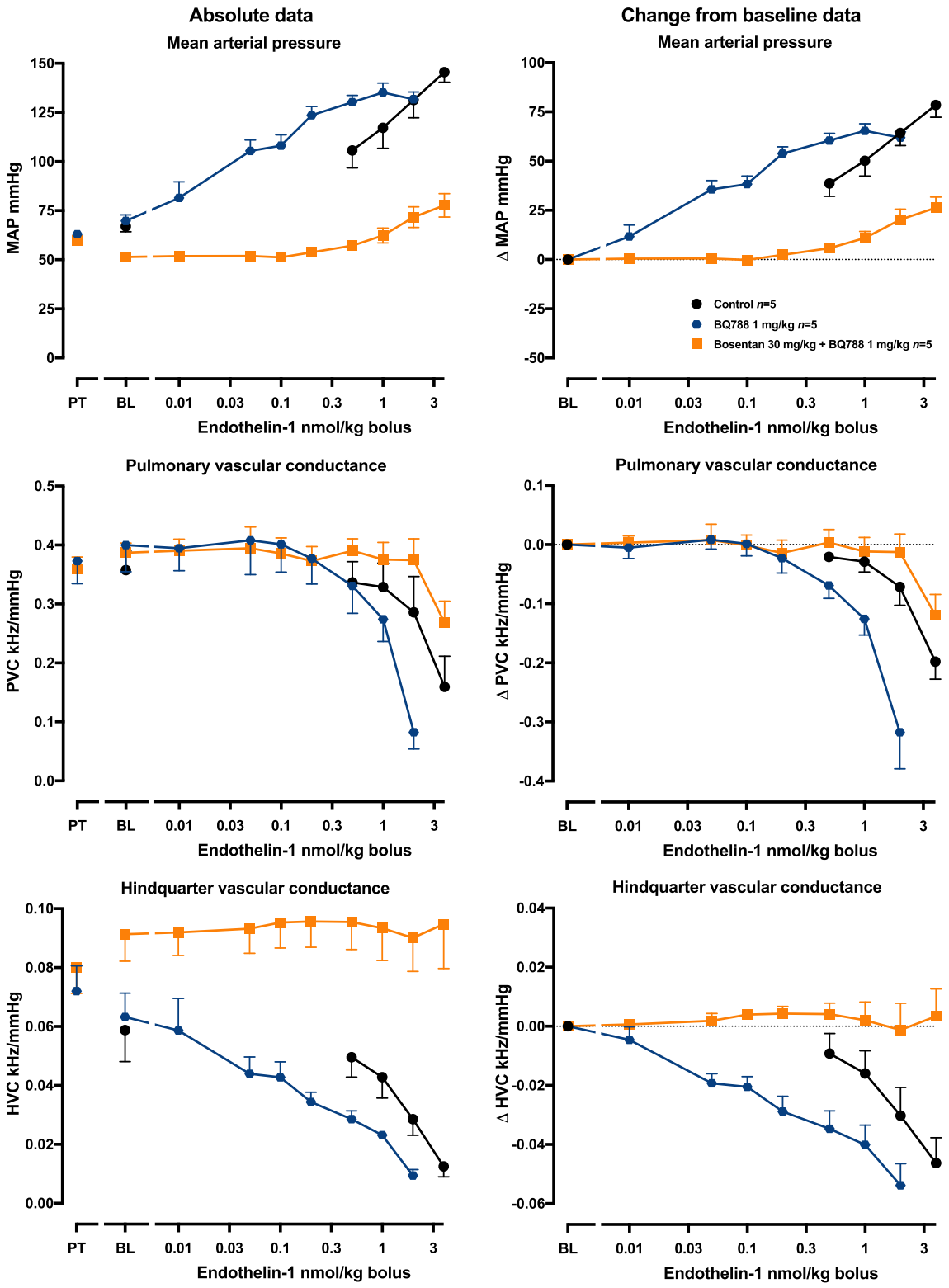

Fig. 4. Effects of the ET_B receptor antagonist BQ788 alone or in combination with bosentan on the mean arterial pressure (MAP, top panels), pulmonary vascular conductance (PVC, middle panels; pulmonary blood flow/pulmonary artery pressure) and hindquarter vascular conductance (HVC, bottom panels; hindquarter blood flow/mean arterial pressure) responses 5 min after each cumulative i.v. bolus injection of endothelin-1 (log scale, x axes). Left panels: PT (pretreatment) is the measurement taken just prior to administration of the treatment (or the equivalent time point in the Control (no pretreatment) group) and BL is the baseline value measured just before injection of the first dose of endothelin-1. There are 3 rat treatment groups (n = 5 each; pretreatments administered i.v. 20 min before the first endothelin-1 dose): Control (no pretreatment); BQ788 1 mg/kg; and BQ788 1 mg/kg combined with bosentan 30 mg/kg. Responses are shown as mean ± S.E.M. in absolute units. Right panels: Change (delta, Δ) values in absolute units from the baseline (BL) just prior to the first cumulative endothelin-1 dose for the metameter in the adjacent left panel.

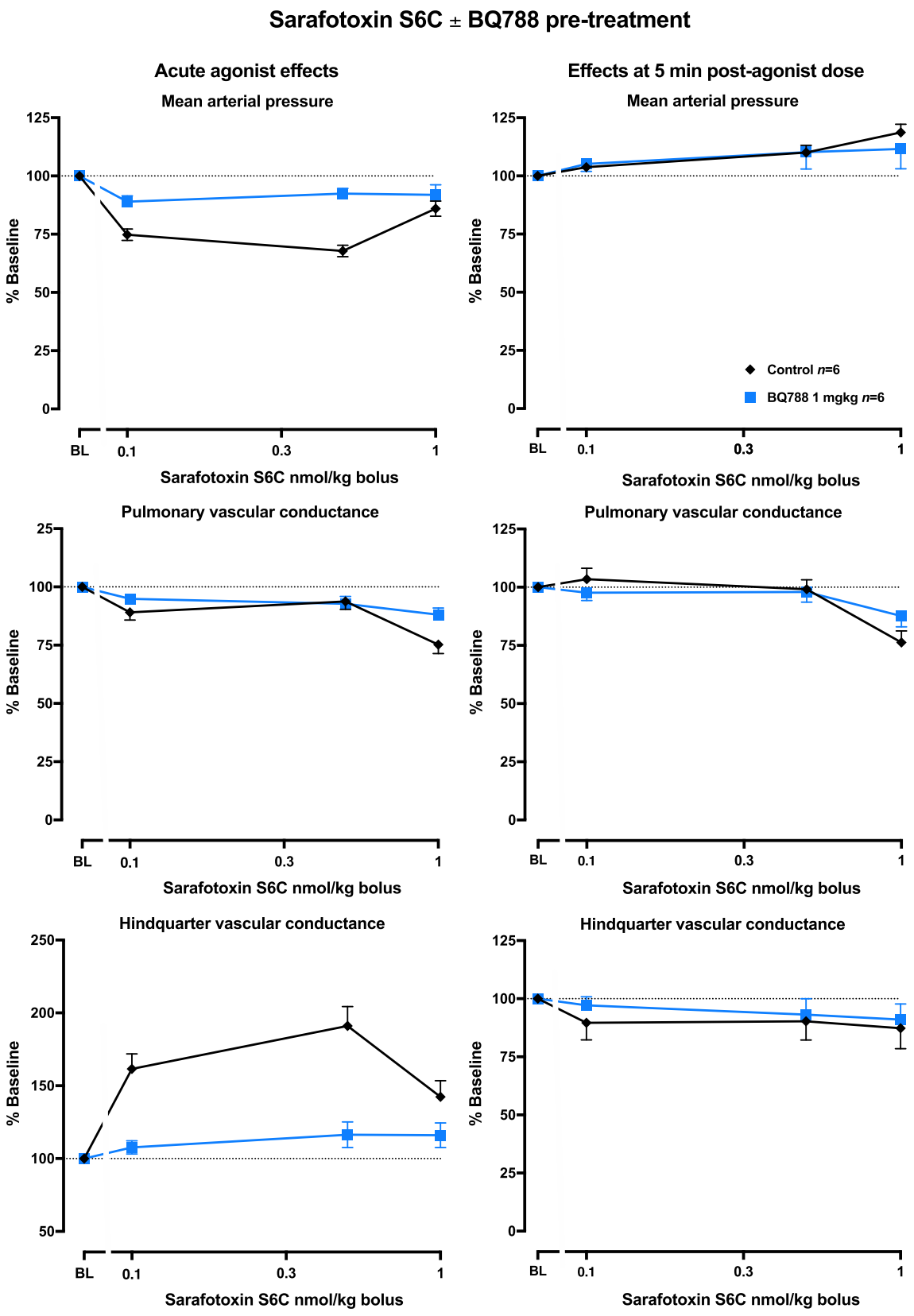

Fig. 5. Effects of the ET_B receptor agonist sarafotoxin S6C alone or in the presence of the ET_B receptor antagonist BQ788 on mean arterial pressure (top panels), pulmonary vascular conductance (middle panels; pulmonary blood flow/pulmonary artery pressure) and hindquarter vascular conductance (bottom panels; hindquarter blood flow/mean arterial pressure); sarafotoxin S6C was administered as cumulative i.v. bolus injections (log scale, x axes). Left panels: Acute (≈0.5–1 min) peak responses to each sarafotoxin S6C bolus dose. Right panels: Measurements at 5 min post-sarafotoxin S6C dose. There are 2 rat treatment groups (n = 6 each; BQ788 administered i.v. 20 min before the first sarafotoxin S6C dose): Control (no pretreatment); and BQ788 1 mg/kg. Responses are shown as mean ± S.E.M., calculated as a percentage (%) of baseline (BL) values measured just before injection of the first dose of sarafotoxin S6C.

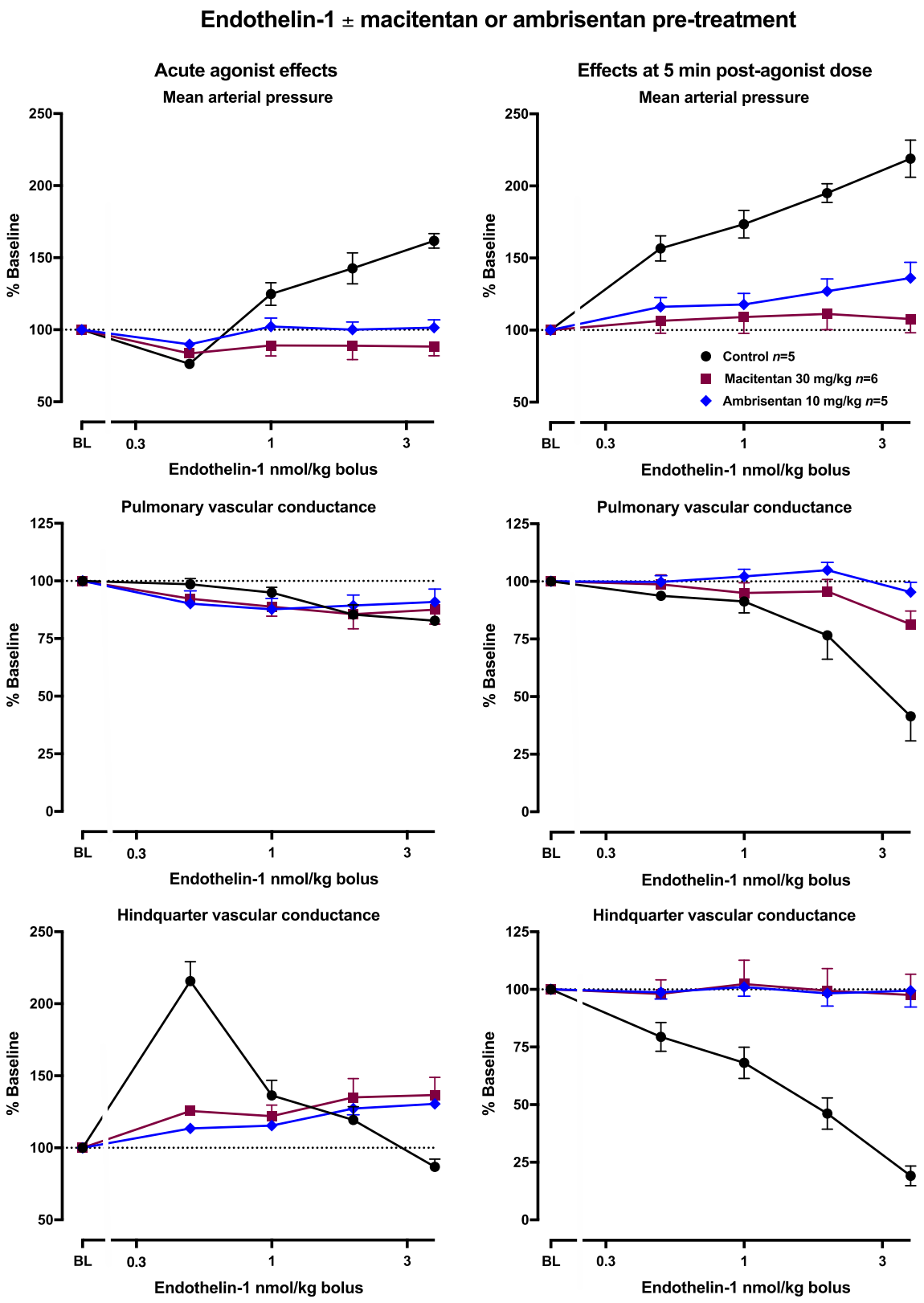

Fig. 6. Effects of the ET_A/ET_B receptor antagonist macitentan or the selective ET_A receptor antagonist ambrisentan on the mean arterial pressure (top panels), pulmonary vascular conductance (middle panels; pulmonary blood flow/pulmonary artery pressure) and hindquarter vascular conductance (bottom panels; hindquarter blood flow/mean arterial pressure) responses to cumulative i.v. bolus injections of endothelin-1 (log scale, x axes). Left panels: Acute (≈0.5–1 min) peak responses to each endothelin-1 bolus dose. Right panels: Measurements at 5 min post-endothelin-1 dose. There are 3 rat treatment groups: Control (no pretreatment, $n = 5$; data repeated from Fig. 2 for comparison); macitentan 30 mg/kg ($n = 6$; administered i.v. 20 min before the first endothelin-1 dose); and ambrisentan 10 mg/kg ($n = 5$; administered i.v. 20 min before the first endothelin-1 dose). Responses are shown as mean ± S.E.M., calculated as a percentage (%) of baseline (BL) values measured just before injection of the first dose of endothelin-1.

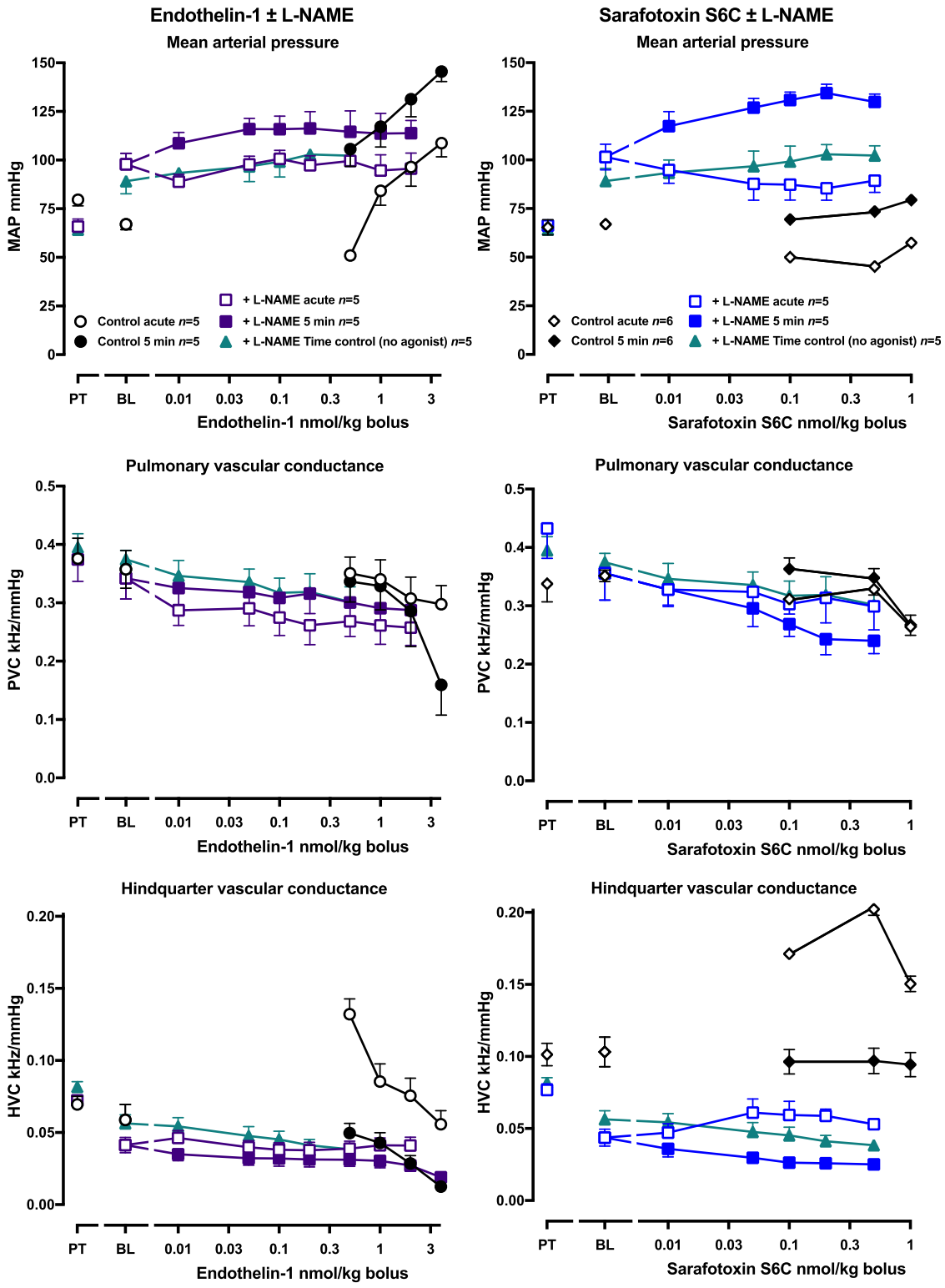

Fig. 7. Mean acute and 5 min post-agonist values for MAP (mmHg), PVC (kHz/mmHg) and HVC (kHz/mmHg) prior to pretreatment (PT) with L-NAME (0.63 mg/kg bolus and 20 mg/kg/h i.v.) and 20 min later during L-NAME treatment (BL). Rats were then administered cumulative bolus injections of (left panels) endothelin-1 or (right panels) sarafotoxin S6C. The Time Control group received L-NAME treatment only (no endothelin-1 or sarafotoxin S6C was administered; data repeated in left and right panels for comparison). There were n = 5–6 rats in each treatment group. Responses are shown as mean ± S.E.M. in absolute units.

in HVC (P = 0.001; Fig. 6, lower left panel). At 5 min after endothelin-1 administration, there was a significant dose-dependent residual small rise in MAP (P = 0.028), suggesting that the ET_A receptor-mediated response was not completely antagonised. The vasoconstriction in the hindquarter and pulmonary vascular beds induced by endothelin-1 was prevented by ambrisentan (Fig. 6, right panels).

3.7. Effects of L-NAME on responses to endothelin-1 or sarafotoxin S6C

Administration of L-NAME (0.63 mg/kg bolus + 20 mg/kg/h

infusion) caused an immediate significant increase in MAP of 25 ± 6 mmHg (+57%); this was sustained and stabilised at an increase of 38 ± 4 mmHg over the time period of the protocol ($P = 0.0017$ within time control group; Fig. 7, upper panels). This effect was consistent with a marked vasoconstriction in the hindquarter vascular bed as HVC fell significantly by −31 ± 8% to −53 ± 4% over the time course ($P = 0.0025$). In contrast, the pulmonary artery pressure was unchanged by L-NAME (Table 1), while PVC still decreased significantly by −11 ± 7% to −19 ± 6% during the protocol ($P = 0.021$, RM ANOVA).

In the presence of L-NAME, the first endothelin-1 bolus dose (0.01 nmol/kg) caused only a small increase in MAP ($P = 0.022$) and further cumulative doses up to 2 nmol/kg did not elicit additional rises (Fig. 7, top left panel). In contrast, in rats not treated with L-NAME, MAP increased sharply by 5 min after endothelin-1 doses of 0.5–4 nmol/kg, as described above (Fig. 7, top left panel). In the pulmonary vascular bed in the presence of L-NAME, 5 min after administration of endothelin-1 (0.01–2 nmol/kg) there were no changes in MAP compared to the baseline ($P = 0.12$; Fig. 7, middle left panel). In the hindquarter vascular bed, the acute (≈1 min) marked vasodilatation response to endothelin-1 was completely inhibited and HVC was significantly decreased at 5 min by endothelin-1 doses from 0.1 to 2 nmol/kg with L-NAME pretreatment (−23 to −52%, $P < 0.05$, RM ANOVA with Dunnett's test; Fig. 7, lower left panel).

Sarafotoxin S6C injection (0.01–0.5 nmol/kg) caused MAP to rise by a further 16–33 mmHg in the presence of L-NAME at 5 min post-administration ($P = 0.016$), in contrast to the lack of significant change in MAP at the acute 1 min time point with any agonist dose ($P = 0.32$; Fig. 7, top right panel). In the pulmonary vascular bed sarafotoxin S6C tended to cause vasoconstriction in the presence of L-NAME, but this did not reach significance ($P = 0.13$, RM ANOVA); PVC responses were comparable with those in the time control group ($P = 0.69$ for the interaction term, RM 2-way ANOVA; Fig. 7, middle right panel). In the hindquarter with L-NAME pretreatment, sarafotoxin S6C administration caused no significant vasodilatation at the acute 1 min time point ($P = 0.14$), in marked contrast to the effects of sarafotoxin S6C in the absence of L-NAME (Fig. 7, lower right panel). However, sarafotoxin S6C caused a further modest vasoconstriction in the presence of L-NAME ($P = 0.011$, RM ANOVA), but the trend line was similar to the time control treatment group ($P = 0.48$ for the interaction term, RM 2-way ANOVA; Fig. 7, lower right panel).

4. Discussion

In this work we demonstrate that the vascular responses to intravenous injection of endothelin-1 are possibly determined by (i) a pulmonary vascular bed clearance mechanism mediated by endothelin ET_B receptors that lowers the circulating concentration of endothelin-1; (ii) endothelin ET_B receptors that release nitric oxide especially in the first min post-injection in the hindquarter vasculature but less obviously in the pulmonary bed; (iii) endothelin ET_A receptors that mediate vasoconstriction in the hindquarter bed; and (iv) a mix of endothelin ET_A and ET_B receptors mediating vasoconstriction in the pulmonary bed (Fig. 8b).

4.1. Endothelin ET_B receptor-selective agonist and antagonist

The effects of the endothelin ET_B receptor-selective agonist sarafotoxin S6C and the endothelin ET_B receptor-selective antagonist BQ788 clearly differentiate the acute vasodilatation of sarafotoxin S6C in the hindquarter vascular bed from the vasoconstriction in the pulmonary bed (Figs. 5 and 8). Importantly, data at 5 min post-injection show there is no change in the hindquarter bed with sarafotoxin S6C up to 1 nmol/kg, ruling out any role for endothelin ET_B receptor-mediated constrictor or dilator activity in this vascular bed. Evidence that the acute hindquarter dilatation was mediated by the endothelin ET_B receptor was shown by the complete block of this response and the fall in MAP by pretreatment with BQ788 1 mg/kg (Fig. 5). This dose of BQ788 has been shown to completely block the depressor response to sarafotoxin S6C 1 nmol/kg i.v. in the pithed rat (Flynn et al., 1995). The endothelin ET_B receptor-mediated hindquarter vasodilatation is most likely due to the endothelial endothelin ET_B receptors causing the release of nitric oxide as this acute response to sarafotoxin S6C was completely blocked by L-NAME (Fig. 7). With nitric oxide blocked by L-NAME treatment, the hindquarter bed was markedly constricted (31% initial fall in HVC) in comparison with the pulmonary bed (11% fall in PVC) at baseline, once more indicating the importance of basal release of nitric oxide to maintain vasodilatation in the hindquarter bed compared with the pulmonary bed (Table 1). Again, the location of endothelin ET_B receptors on pulmonary artery smooth muscle but not endothelial cells allowed for the sarafotoxin S6C-mediated constriction in the pulmonary bed (Figs. 5, 7 and 8b). L-NAME treatment may also cause a rise in plasma big endothelin-1 but not immunoreactive endothelin-1 in anaesthetised rabbits. Importantly, BQ788 still caused a similar near doubling of immunoreactive endothelin-1 levels in the presence or absence of L-NAME (Gratton et al., 1997).

4.2. Bosentan, macitentan and ambrisentan

In dose-finding experiments it was important to establish what dose of bosentan was required to antagonise the effects of endothelin-1 up to 4 nmol/kg. As indicated in Fig. 2, the highest dose of bosentan tested (30 mg/kg i.v.) was sufficient to completely inhibit the acute effects of endothelin-1 on MAP, PVC and HVC. For the 5 min time point, bosentan 30 mg/kg did significantly block the increase in MAP, though there appeared to be a residual pressor response as previously observed in pithed rats (Clozel et al., 1994). However, this antagonist dose was sufficient to inhibit the falls in PVC and HVC (Fig. 2).

From binding studies on human cloned receptor assays, ambrisentan is reported to be an endothelin ET_A receptor-selective antagonist of more than 200-fold over endothelin ET_B receptors (Spence et al., 2008). However, our work and that of others show that this apparent binding selectivity is much decreased when assayed functionally to approximately 32-fold; a similar selectivity ratio as observed for bosentan (25-fold) and macitentan (50-fold) (Angus et al., 2017a, 2017b; Iglarz et al., 2008). Indeed, the similarity between the inhibitory effects of ambrisentan or macitentan on the haemodynamic responses to endothelin-1 *in vivo* is clearly shown in Fig. 6.

4.3. Clearance of endothelin-1

It is important to bring together findings from the *in vitro* isolated artery experiments with these *in vivo* results noting that isolated arteries are but one segment of the vasculature and *in vivo*, the entire vascular/resistance bed contributes to the measurement of vascular reactivity. Nevertheless, our previous rat isolated pulmonary small artery experiments suggested that this 300 μm i.d. small resistance artery constricts to endothelin-1 but the concentration-response curve is LEFT-shifted by the endothelin ET_B receptor antagonist BQ788 that is independent of nitric oxide (Angus et al., 2017a). Similarly, we found here that the pretreatment with BQ788 not only abolished the probable nitric oxide-dependent increase in HVC, but potentiated the vasoconstriction elicited by endothelin-1 in the pulmonary and hindquarter vascular beds.

There was a similar result in the rat isolated small pulmonary artery, but not in the rat isolated mesenteric artery (Angus et al., 2017a). The important difference is that the i.v. administered endothelin-1 must first pass through the lungs – where the clearance of endothelin-1 occurs before/at the pulmonary vasculature – and then on into the arterial circulation such as the hindquarter vasculature. Thus, in the pulmonary vasculature the clearance of endothelin-1 locally affects the concentration of endothelin-1 presented to the small pulmonary artery resistance vessels, whereas in the hindquarter vasculature the distant,

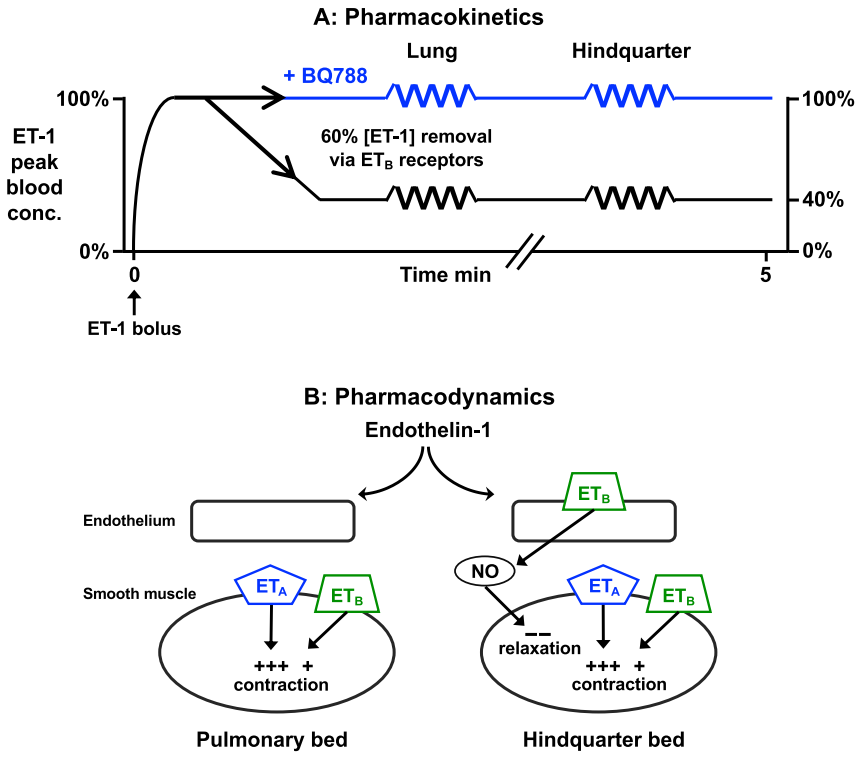

Fig. 8. Top panel A: Schema to illustrate the pharmacokinetic effect of the endothelin-1 clearance mechanism mediated by endothelin ET_B receptors in the lung vasculature. At bolus injection i.v. of endothelin-1, the endothelin-1 peak blood concentration, initially 100%, then falls to 40% due to pulmonary clearance before the constrictor effects are observed in the lung and hindquarter vasculature. This clearance mechanism is blocked by BQ788. Bottom panel B: Schema to illustrate the location of receptors involved in the acute and 5 min effects of endothelin-1 in the pulmonary (left) and hindquarter (right) vascular beds. Nitric oxide (NO) is released acutely in the hindquarter bed via ET_B receptors, while ET_A and ET_B receptors mediate vasoconstriction in both hindquarter and pulmonary beds at 5 min post-injection of endothelin-1.

upstream lung clearance of endothelin-1 presents a shift in endothelin-1 sensitivity *in vivo* – clearly an effect that would not be observed in isolated arteries (Fig. 8a).

Rather than directly measure the endothelin-1 concentration before and after BQ788 we have a readout of the increase in sensitivity to exogenous endothelin-1 from the left-shift in the dose-response curves. We calculated a 2.5-fold increase in potency in the PVC and a similar 2.4-fold increase in the HVC in the presence of BQ788. So, when the endothelin ET_B receptor-mediated removal is present, the effective functional concentration of endothelin-1 is 1/2.5, i.e. 0.4 or a loss of 0.6 or 60% (Fig. 8a). These functional studies in anaesthetised rats directly compare with 5 min post-injection perfusate levels of endothelin-1 in rat isolated perfused lungs where the endothelin-1 concentration rose 4-fold after treatment with the endothelin ET_B receptor antagonist BQ788 (Sato et al., 1995). Further, in mice, either specific endothelial cell knockout of the endothelin ET_B receptor or a selective endothelin ET_B antagonist caused the blood concentration of I^{125}-endothelin-1 to increase by 3-fold (Kelland et al., 2010).

Implications of this *in vivo* study are that there are, at least in the rat pulmonary vasculature, a proportion of endothelin ET_B receptors that mediate vasoconstriction that is not observed in the hindquarter vasculature. The consequences of this fact are that endothelin ET_B receptor antagonists may well inhibit a proportion of the vasoconstrictor actions of endothelin-1, but equally, endothelin ET_B antagonists will inhibit the endothelin ET_B receptor-mediated uptake and clearance of endothelin-1 in the lung. We found that this clearance mechanism, when blocked by endothelin ET_B receptor antagonism, can potentiate the endothelin-1 dose-response curve by up to 3-fold in both the pulmonary and hindquarter vasculature; a significant sensitisation to endothelin-1.

4.4. Implications

The implications for treatment of endothelin-1-mediated pulmonary vasoconstriction and pulmonary artery hypertension are that a selective endothelin ET_A receptor antagonist is preferable to a truly mixed, i.e. equally active endothelin ET_A/ET_B receptor antagonist. We argue again (for more detail, see Angus et al., 2017a) that the "ideal" endothelin-1 antagonist for pulmonary artery hypertension should have an endothelin ET_B:ET_A receptor selectivity ratio of at least 3:1 to ensure there is not only antagonism of the clearance mechanism but also of the vasoconstrictor actions at the endothelin ET_A and ET_B receptors active in pulmonary small arteries.

Conflicts of interest

None.

Acknowledgements

We are indebted to the excellent technical assistance of Ms Linda Cornthwaite-Duncan.

This research did not receive any specific grant from funding agencies in the public, commercial, or not-for-profit sectors.

References

Angus, J.A., Hughes, R.J.A., Wright, C.E., 2017a. Distortion of K_B estimates of endothelin-1 ET_A and ET_B receptor antagonists in pulmonary arteries: possible role of an endothelin-1 clearance mechanism. Pharmacol. Res. Perspect. 5. https://doi.org/10.1002/prp2.374.

Angus, J.A., Soeding, P.F., Hughes, R.J.A., Wright, C.E., 2017b. Functional estimation of endothelin-1 receptor antagonism by bosentan, macitentan and ambrisentan in human pulmonary and radial arteries *in vitro*. Eur. J. Pharmacol. 804, 111–116.

Clozel, M., Breu, V., Gray, G.A., Kalina, B., Loffler, B.M., Burri, K., Cassal, J.M., Hirth, G., Muller, M., Neidhart, W., et al., 1994. Pharmacological characterization of bosentan, a new potent orally active nonpeptide endothelin receptor antagonist. J. Pharmacol. Exp. Ther. 270, 228–235.

Colquhoun, D., 1971. Lectures on Biostatistics. Oxford University Press, Oxford, pp. 311–319.

de Nucci, G., Thomas, R., D'Orléans-Juste, P., Antunes, E., Walder, C., Warner, T.D., Vane, J.R., 1988. Pressor effects of circulating endothelin are limited by its removal in the pulmonary circulation and by the release of prostacyclin and endothelium-derived relaxing factor. Proc. Natl. Acad. Sci. U. S. A. 85, 9797–9800.

Dupuis, J., Goresky, C.A., Fournier, A., 1996. Pulmonary clearance of circulating endothelin-1 in dogs in vivo: exclusive role of ET_B receptors. J Appl Physiol 81, 1510–1515 (1985).

Flynn, D.A., Sargent, C.A., Brazdil, R., Brown, T.J., Roach, A.G., 1995. Sarafotoxin S6c elicits a non-ET_A or non-ET_B-mediated pressor response in the pithed rat. J. Cardiovasc. Pharmacol. 26 (Suppl. 3), S219–S221.

Fukuroda, T., Fujikawa, T., Ozaki, S., Ishikawa, K., Yano, M., Nishikibe, M., 1994.

Clearance of circulating endothelin-1 by ET_B receptors in rats. Biochem. Biophys. Res. Commun. 199, 1461–1465.
Gardiner, S.M., Kemp, P.A., Bennett, T., 1993. Regional haemodynamic responses to intravenous and intraarterial endothelin-1 and big endothelin-1 in conscious rats. Br. J. Pharmacol. 110, 1532–1536.
Gratton, J.P., Cournoyer, G., Löffler, B.M., Sirois, P., D'Orléans-Juste, P., 1997. ET_B receptor and nitric oxide synthase blockade induce BQ-123-sensitive pressor effects in the rabbit. Hypertension 30, 1204–1209.
Iglarz, M., Binkert, C., Morrison, K., Fischli, W., Gatfield, J., Treiber, A., Weller, T., Bolli, M.H., Boss, C., Buchmann, S., Capeleto, B., Hess, P., Qiu, C., Clozel, M., 2008. Pharmacology of macitentan, an orally active tissue-targeting dual endothelin receptor antagonist. J. Pharmacol. Exp. Ther. 327, 736–745.
Johnstrom, P., Fryer, T.D., Richards, H.K., Harris, N.G., Barret, O., Clark, J.C., Pickard, J.D., Davenport, A.P., 2005. Positron emission tomography using 18F-labelled endothelin-1 reveals prevention of binding to cardiac receptors owing to tissue-specific clearance by ET B receptors in vivo. Br. J. Pharmacol. 144, 115–122.
Kelland, N.F., Kuc, R.E., McLean, D.L., Azfer, A., Bagnall, A.J., Gray, G.A., Gulliver-Sloan, F.H., Maguire, J.J., Davenport, A.P., Kotelevtsev, Y.V., Webb, D.J., 2010. Endothelial cell-specific ET_B receptor knockout: autoradiographic and histological characterisation and crucial role in the clearance of endothelin-1. Can. J. Physiol. Pharmacol. 88, 644–651.
Reinhart, G.A., Preusser, L.C., Burke, S.E., Wessale, J.L., Wegner, C.D., Opgenorth, T.J., Cox, B.F., 2002. Hypertension induced by blockade of ET_B receptors in conscious nonhuman primates: role of ET_A receptors. Am. J. Physiol. Heart Circ. Physiol. 283, H1555–H1561.
Sato, K., Oka, M., Hasunuma, K., Ohnishi, M., Sato, K., Kira, S., 1995. Effects of separate and combined ET_A and ET_B blockade on ET-1-induced constriction in perfused rat lungs. Am. J. Physiol. 269, L668–L672.
Spence, R., Mandagere, A., Dufton, C., Venitz, J., 2008. Pharmacokinetics and safety of ambrisentan in combination with sildenafil in healthy volunteers. J. Clin. Pharmacol. 48, 1451–1459.
Weber, C., Schmitt, R., Birnboeck, H., Hopfgartner, G., van Marle, S.P., Peeters, P.A., Jonkman, J.H., Jones, C.R., 1996. Pharmacokinetics and pharmacodynamics of the endothelin-receptor antagonist bosentan in healthy human subjects. Clin. Pharmacol. Ther. 60, 124–137.